

MODELING OF GRAIN PULLOUT IN FATIGUED POLYCRYSTALLINE ALUMINA

M.T. Kokaly¹, A.S. Kobayashi¹ and K.W. White²

¹University of Washington, Department of Mechanical Engineering, Seattle, WA 98195-2600, USA

²University of Houston, Department of Mechanical Engineering, Houston, TX 77204-4792, USA

ABSTRACT

A second generation, 2-D finite element (FE) model of grain pull-out and push-in in an alumina wedge-opening double cantilever beam (WL-DCB) specimen was constructed using observations and measurements from photomicrographs of the specimen surface. The FE model consisted of an idealized structure of quadrilateral elements corresponding to three different grain sizes. Frictional sliding, intact elastic grains, and cantilever grains were modeled in the interface. The observed intragranular fracture sites and appearance of detached grains indicative of broken elastic grain bridges and rotated grains were included in the model by removing the relevant elements. An iterative inverse process was used to match the experimental cyclic load/unload test results of the WL-DCB specimen.

KEYWORDS

Inverse analysis, hybrid experimental-numerical analysis, ceramic fracture, low cycle fatigue, fracture process zone.

INTRODUCTION

Since the earlier work of Knehans et. al. [1], numerous work on the toughening effects generated by grain bridging in the trailing fracture process zone (FPZ) have been published, especially over the last decade. Unfortunately, the controlling factor, the grain bridging force was only inferred in the majority of studies. Hay and White [2] used a “post fracture tension” (PFT) specimen to directly measure the crack closure stresses (CCS) in the trailing wake of a stably grown crack in a high purity alumina double cantilever beam (WL-DCB) specimen. The PFT results provided an excellent platform for modeling the grain-bridging force due to frictional sliding since other grain bridging mechanisms such as elastic grain bridging and cantilevered grain rotation occur only immediately in front of the crack tip. A zero order finite element (FE) model of the PFT specimen subjected to monotonic loading by Tran, et. al. [3] provided the load versus displacement results which were in remarkable agreement with the measured results of [2]. This modeling was followed by a first order FE model [4] of a cyclically loaded PFT specimen based on the newer results of Hay and White

[5]. In this paper, we present a second order FE model of grain bridging in a cyclically wedge-loaded double cantilever beam (WL-DCB) specimen.

EXPERIMENTAL BACKGROUND

A high purity alumina (Coors AD998), WL-DCB specimen was cyclically loaded under displacement control at room temperature, 600, and 800°C. The applied load and the crack opening displacement (COD) profile, determined through moiré interferometry, were recorded during the loading and unloading processes. Details of the experimental procedure and results are given in [6].

The crack opening profiles at the maximum and minimum loads during the first loading cycle at room temperature are shown in Fig. 1. Comparison of the loaded and unloaded crack opening profiles revealed not only a residual crack opening along the length of the crack but a residual crack opening larger than that at the maximum load in the area near the crack tip. The residual crack opening was attributed to a cantilever effect from the interference of completely pulled out grain bridges during unloading. The residual COD at unloading was found to increase after the next cycle of loading. This increase in residual COD and the related decrease in sliding distance between frictional grains was the probable cause of the lack of fatigue damage and hence fatigue crack extension in tension-tension cycling of monolithic structural ceramics in an inert environment.

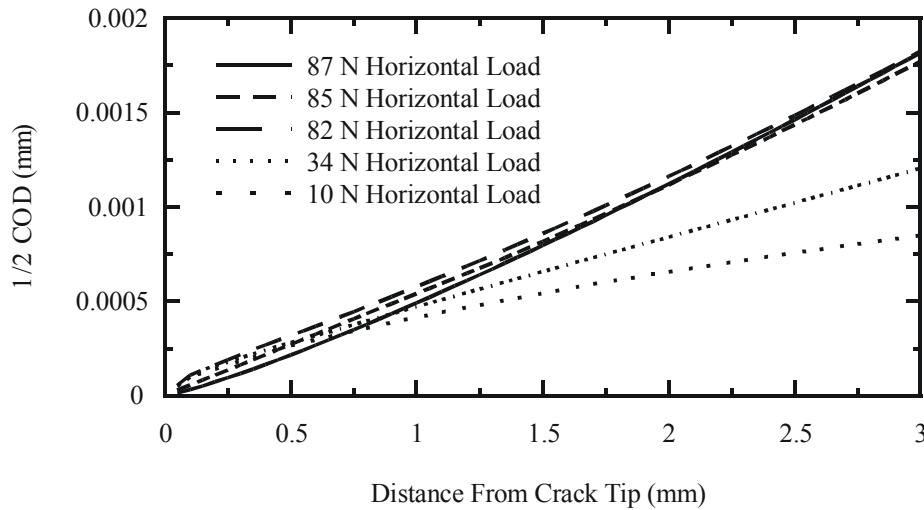


Fig. 1. Crack profiles at 1st loading cycle.

Side-surface Micrograph

Figures 2 and 3 show the micrographs along a crack in the side surface of a WL-DCB specimen at unloading after 25 cycles of loading. Intergranular fracture dominated the crack interface and was interspersed with transgranular fracture (in the brackets) in Fig. 2. Although the crack paths in Fig. 3 suggest locations of possible angled grain rotation, most angled grains failed by intergranular fracture prior to an appreciable crack opening. Crack opening at the peak load was resisted by elastic bridges, cantilevered grains, and frictional bridging grains. Elastic grain bridges and cantilevered grains fractured transgranularly or detached from surrounding grains at a small COD after which frictional bridges dominated the resistance to crack opening. An example of a transgranularly fractured grain is given in the highlighted section of Fig. 3. The frictional forces were generated by the residual compressive stresses caused by the anisotropic thermal contraction in the grains during cool down from the processing temperature of 1500°C.

FPZ MICROMECHANICS

Crack Closing (Bridging) Stress

Abundant experimental evidence [1-6] show that the dominant fracture energy dissipation mechanism in structural ceramics is the crack opening resistance in the trailing FPZ of a crack. The FE model described in [3, 4] simplifies the complex micro-mechanics governing grain separation along the opening crack in order to determine the CCS versus COD relation using the experimentally determined load and displacement boundary conditions. A slightly different version of this hybrid analysis was performed to determine the

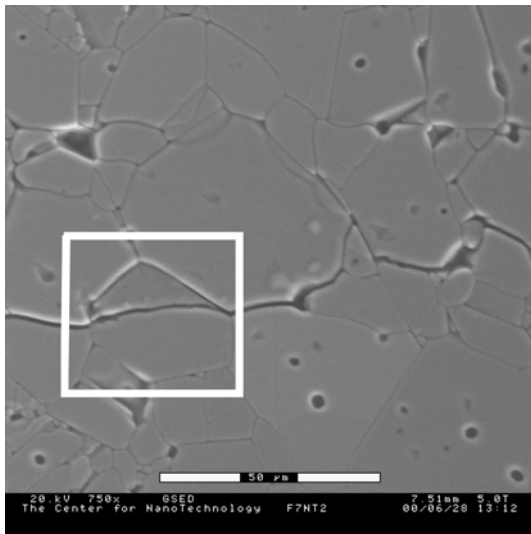


Fig. 2. Intergranular and transgranular cracks.

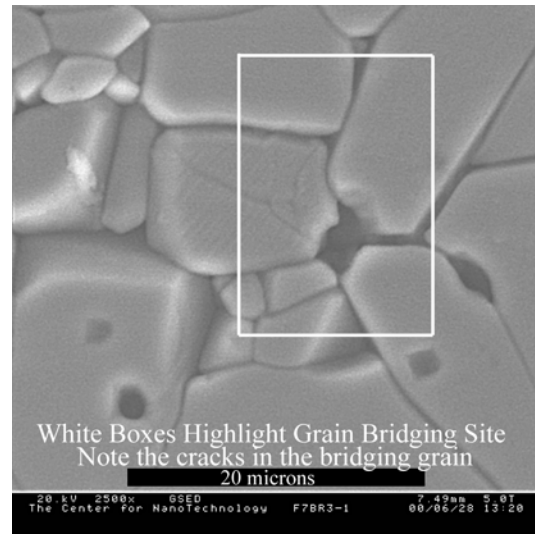


Fig. 3. Fractured bridging grain.

crack closing stress during periods of loading and unloading [6]. Figure 4 shows the difference between the experimentally determined CCS versus COD relations at the maximum applied load at both room temperature and 800°C. The decrease in the crack bridging force at 800°C is attributed to both the decrease in viscosity of the glassy grain interface and the partial relieving of the residual compressive stresses, hence, the decrease in the resistance to grain pullout.

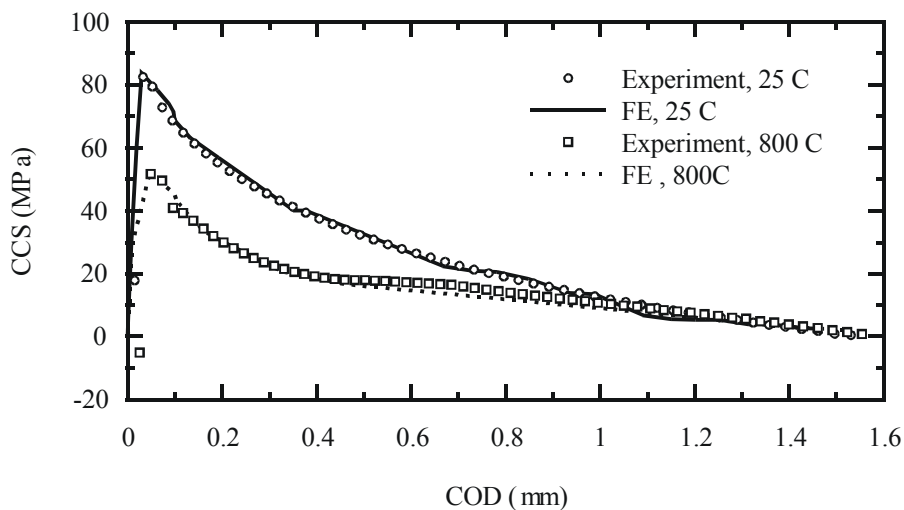


Fig. 4. CCS versus COD relations at maximum load.

FE MODEL

A micromechanical model based on all three grain bridging mechanisms mentioned previously was subjected to the loading cycle. The disposable parameters in the model were the relative contributions of elastic grain bridges, cantilevered grains, and frictional bridging to the grain bridging force [7]. By necessity, the model was a highly idealized assembly of quadrilateral elements. At the interface, elastic grain bridges were modeled by constraining the coincident nodes on the opposite side of the crack to have the same displacement. Angled, cantilevered grains were modeled by adjusting the nodal points of the initial mesh to provide an angled interaction surface. Frictional bridges were modeled, as in the previous cases, with the frictional properties defined at the crack interface. Examples of each type of bridge is given in Fig. 5. Lacking any prior analysis of the behavior of the grain bridges during loading, a time consuming trial-and-

error, iterative inverse analysis was used to match the meso-responses of the micro-mechanical model and the experimental data, primarily the applied load, COD profile and CCS vs. COD relation.

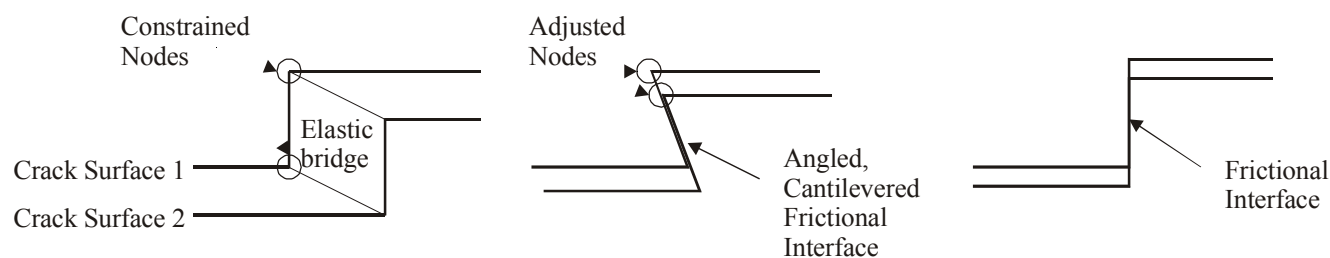


Fig. 5. Modeling of Three Types of Grain Bridges.

The FE model used in this study accounted for the random grain size distribution and the random orientation of the axes of thermal expansion. Unlike previous studies [3, 4], as shown in Fig. 6, this is a two-dimensional idealization of the complex three-dimensional complex distribution of grains through the thickness of the WL-DCB specimen. Since the model was a slice through the thickness of the WL-DCB specimen, the width of the FE model was equal to the thickness of the WL-DCB specimen minus the side groove or 2.4mm. The thickness of the model was equated to the average grain size of 15 μm . A Matlab preprocessor randomly distributed the principal thermal expansion directions from 0 to 160° in 15° increments. The compressive residual stress, which caused frictional resistance to the grain pullout, was generated by the mismatch in grain shrinkage during the cool down from the processing temperature. The complex distributions of irregular grains of various sizes were replaced by trapezoidal and rectangular grains of varying sizes in the region adjacent to the fracture surface as shown in Fig. 6. In order to conserve computing time, three layers of increasingly larger elements with randomly orientated anisotropic thermal coefficients of expansion, were used outside of the fracture region. Grain sizes under 3 μm were considered too small for effective grain bridging in the WL-DCB specimen.

The grain size distribution was incorporated into the model by manipulating the coefficients of thermal expansion. The coefficients were scaled by the ratio of the assigned grain size to the average grain size of 15 μm . This allowed the model to maintain a reasonable residual thermal strains and hence residual compressive stresses between grains while using a simple mesh. Since the goal of the model involved the interactions between grains, a surface area grain distribution was used. This retained the distribution of expansion mismatch between grains as in the real material and hence, residual stress at the interface.

Material Properties

The linear coefficients of thermal expansion in the two principle directions were assumed to be 8.62×10^{-6} in the (0001) plane and 9.38×10^{-6} mm/°C in the [0001] direction. Because of the existence of a symmetry plane, 1/3 of the grains were assigned an isotropic thermal expansion equal to the expansion in the (0001) plane. An isotropic modulus of elasticity of 350 GPa and a Poisson ratio of 0.23 were used. The elastic isotropy assumption was based justified on the basis of [8], which showed, by a numerical experiment, that the effect of elastic anisotropy of the alumina grains had negligible effect on the average residual stresses, which were generated by thermal anisotropy.

In the absence of any micro-mechanical data, the friction coefficient for estimating the resistance to the subsequent intergranular sliding was assumed to be 0.7. The Coulomb friction coefficient was an educated average of the bulk friction coefficients given by Jahanmir and Dong [9] and was adjusted to account for the rougher surfaces due to the presence of the interstitial phase.

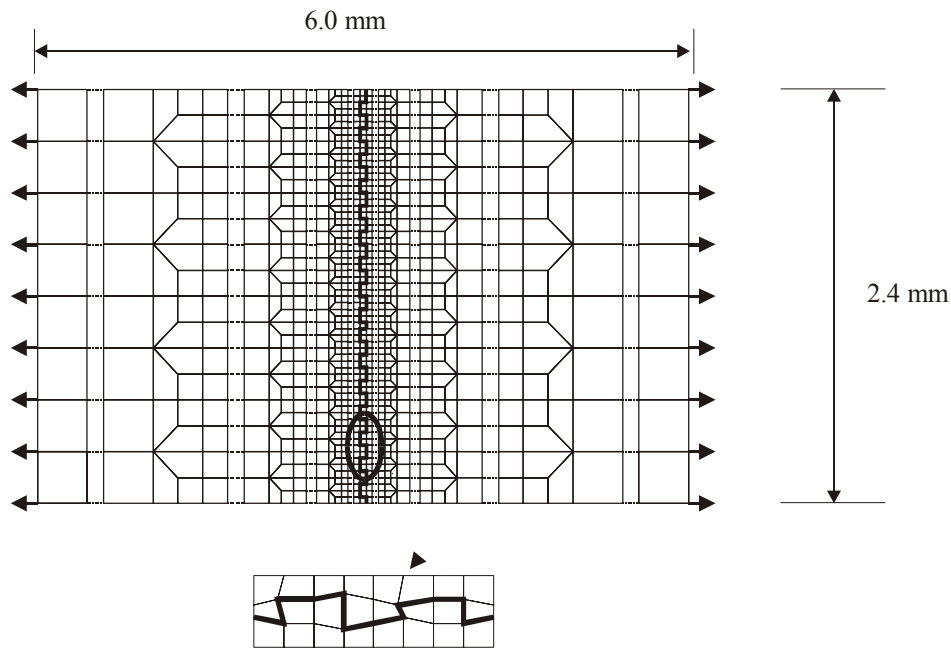


Fig. 6. FE model of the fracture surface.

RESULTS

Initially, the FE model was subjected to a cool down process from 1500°C to 25°C or 800°C. The model was then subjected to a cyclic loading. The relative contributions of the various bridging mechanisms to the CCS were adjusted to match the CCS versus COD relation. The resulting CCS vs. COD relations generated by the FE model are shown in Fig. 4 together with the corresponding experimental data. The computed and measured unloading CCS vs. COD relations at locations 0.1, 1.0 and 2.0 mm from the crack tip are also shown in Figs. 7 and 8. In all cases, the COD did not return to zero. These results show that additional compressive force is required to return the grains to their original uncracked position. Furthermore, the good agreement of the FE results and the experimental data indicates that the assumptions and modeling techniques used were successful in representing the micro-mechanics of grain bridging in alumina during loading and unloading.

CONCLUSION

A micro-mechanical FE model, which is based on grain pullout and push-in of a WL-DCB specimen has been presented. The FE model, which was developed through an inverse process, successfully replicated the measured cyclic load and unload relations of an alumina WL-DCB specimen.

ACKNOWLEDGMENT

The work reported here is supported by an AFOSR grant F49620-96-1-0451, Dr. Ozden Ochoa, was the grant monitor.

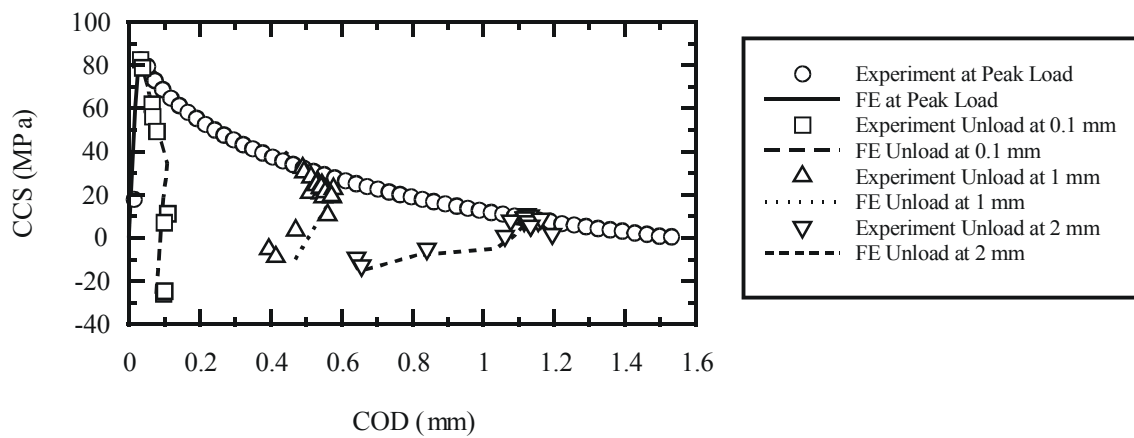


Fig. 7. CCS vs. COD relations during the first loading and unloading at room temperature.

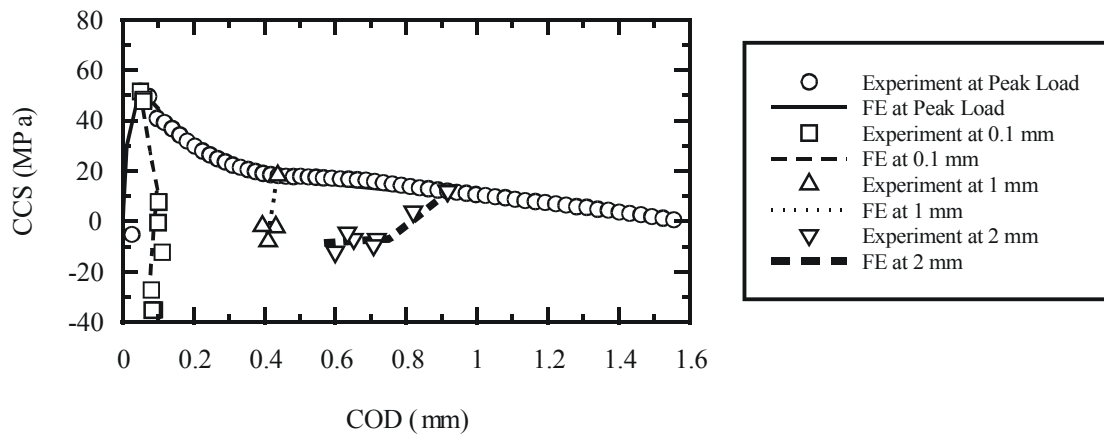


Fig. 8. CCS vs. COD relations during the first loading and unloading at 800° C.

REFERENCES

- [1] R. Knehans and R.W. Steinbrech, *J. Matr. Sci. Lett.* **1** (8) (1982), 327.
- [2] J.C. Hay. and K.W. White, *J. Am. Ceram. Soc.* **78** (1995), 1025-1032.
- [3] D.T. Tran, C.T. Yu, J.C. Hay, K.W.White and A.S. Kobayashi, in *Fracture Mechanics of Ceramics 11*, R.C. Bradt, D.P.H. Hasselman, D. Munz, M. Sakai and V. Ya Shevchenko, eds, Plenum Publishing Corp. (1996), 29.
- [4] M.T. Kokaly, D.K. Tran, A.S. Kobayashi, X. Dai, K. Patel and K.W. White, *Mat'l Sci. Eng. A285* (2000), 151.
- [5] J.C. Hay and K.W.White, *Acta mater.* **45** (9) (1997), 3625.
- [6] Kokaly, M.T., Kobayashi, A.S. and White, K.W. in *Proc. of Int'l. Conf. Fracture 10*, Honolulu, HI, Dec. 3-7, 2001.
- [7] G. Vekinis, M.F. Ashby and P.W.R. Beumont, *Acta. Metall. Mater.*, **38** (600), 1151-1162.
- [8] A.F. Bower and M. Ortiz, *ASME J. Engr. Mater. Techn.* **115** (2) (1993), 230.
- [9] S. Jahanmir and X. Dong, *J. Tribology* **114** (1992), 403.